Accurate Determination of the Ordinary Index Profile of Proton-Exchanged Waveguides

M. Marangoni, R. Ramponi, R. Osellame, and V. Russo

***Abstract*—A new method for an accurate characterization of the ordinary refractive index profile of proton-exchanged waveguides is presented and discussed. The method is based on the measurement of the power coupled into radiation modes of the waveguide as a function of the corresponding effective indexes, and allows the determination of the depth and of the film refractive index of the ordinary profile by a least squares fitting of the experimental points. The depth and the film refractive index have been experimentally obtained with an accuracy of 0.005 μm and 0.0001, respectively.**

***Index Terms*—Integrated optics, optical device fabrication, optical planar waveguides, optical planar waveguide couplers, optical propagation in anisotropic media, optical propagation in nonlinear media, optical variables measurement, optical waveguide theory.**

I. Introduction

IN THE last few years, proton-exchanged (PE) $LiNbO_3$ waveguides have attracted an increasing interest thanks to their potentialities in different application domains, such as integrated lasers [1] and optical frequency conversion devices [2]. As it is well known, proton exchange increases the extraordinary refractive index of $LiNbO_3$ while it decreases the ordinary one [3], thus allowing the propagation of only guided extraordinary modes. Nevertheless, the knowledge of the ordinary refractive index profile is of great importance to determine different aspects of the modeling of PE waveguides, such as the crystallographic phase of the exchanged layer [4], the time evolution of the optical properties as a function of the annealing time [5], and the propagation conditions of transverse magnetic (TM)-polarized modes in Z-cut waveguides [6].

Owing to the negative ordinary refractive index change, and thus to the lack of ordinary guided modes, conventional m-lines spectroscopy cannot be used for the determination of the ordinary profile. To overcome this problem, three different methods have been proposed in the literature, exploiting i) the realization of a reverse PE layer [7], ii) the use of a spectrophotometer for the determination of the transmission spectrum of the exchanged layer [5], and iii) the application of a dark-mode reflectivity technique [8], [9]. None of these methods allows the determination of the ordinary film refractive index (n_f) and of the film depth (w) with an accuracy better than 0.001 and 0.05 μm, respectively.

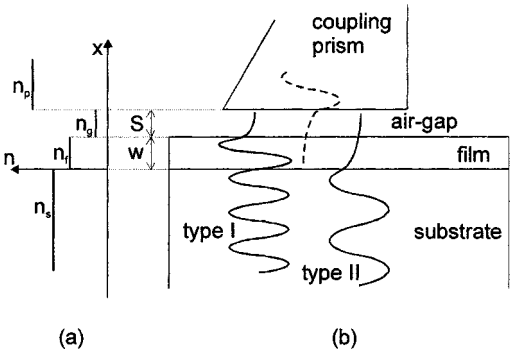

Fig. 1. (a) Dielectric structure of a prism-coupler when the ordinary refractive index profile of a PE waveguide is taken into account. (b) Field profile of the incoming beam (dashed line) and of the coupled radiation mode (continuous line). Type I occurs for $n_g < n_{\text{eff}} < n_f$, type II for $n_f < n_{\text{eff}} < n_s$. S is the air–gap spacing; w is the film depth.

In this paper, a new method is presented and discussed, that allows the determination of both parameters with an accuracy improved by an order of magnitude by exploiting the Fabry–Perot effect in the waveguide film. The method requires prism-coupling of the ordinary radiation modes of the waveguide and the determination of the coupled power behavior as a function of the effective refractive indexes of the radiation modes themselves. The curve representing the coupled power versus the effective indexes typically shows the interference fringes given by the light reflected back and forth in the waveguide film. The interference peaks are generally not sharp, so that, if only the positions of maxima and minima are considered for the ordinary index-profile reconstruction [9], an accuracy better than 0.001 on n_f and 0.05 μm on w cannot be achieved. On the contrary, if the full behavior of the coupled power is fitted with a theoretical curve, as calculated by extending the classical theory of prism coupling [10] to radiation modes, the accuracy of the reconstructed optical parameters is greatly enhanced. Experimental confirmation of the accuracy of the method proposed here has been obtained by comparing the depth of the extraordinary index profile as obtained by standard m-lines spectroscopy, with the depth of the ordinary index profile, both corresponding to the depth of the waveguide film: an agreement within 0.005 μm has been found.

II. Operating Principle

The ordinary refractive index profile of a PE planar waveguide can be well approximated by a step-index profile [11] as

Manuscript received January 26, 2000; revised May 19, 2000. This work was supported in part by the National Project CNR-MADESS II and the INFM-PAIS "Frequency shifting and amplification of optical signals through cascaded second-order processes in optical waveguides."

The authors are with the Istituto Nazionale Fisica della Materia (INFM), Dipartimento di Fisica-Politecnico and Centro di Elettronica Quantistica e Strumentazione Elettronica (CEQSE) del Consiglio Nazionale delle Ricerche (CNR), 20133 Milan, Italy (e-mail: roberta.ramponi@polimi.it).

Publisher Item Identifier S 0733-8724(00)08081-6.

0733–8724/00$10.00 © 2000 IEEE

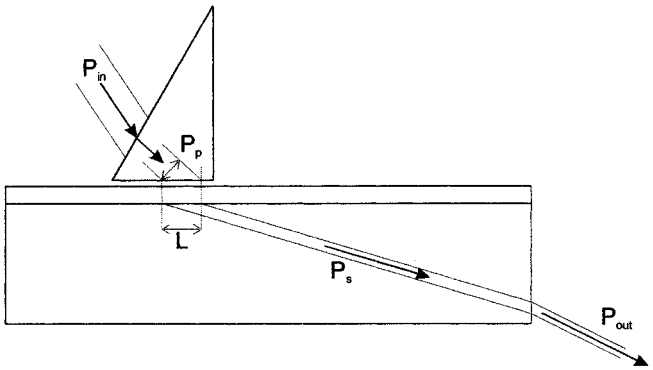

Fig. 2. Optical powers involved in the radiation modes prism-coupling. L = length of the coupling region.

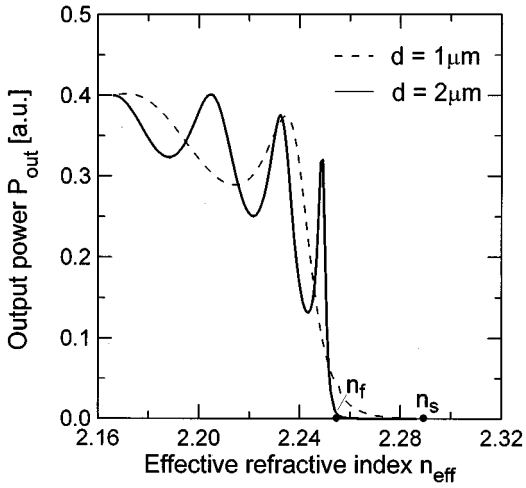

Fig. 3. Theoretical curves relating the power P_{out} coupled into ordinary radiation modes of a 1 μm (dashed line) and 2 μm (solid line) deep PE waveguide as a function of the corresponding n_{eff}. Filled circles indicate the film and the substrate refractive indexes n_f and n_s.

shown in Fig. 1(a), where the film ordinary refractive index n_f is lower than the substrate ordinary index n_s. Such a dielectric structure does not support any guided mode and thus cannot be characterized through conventional m-lines spectroscopy. However, an accurate characterization is still possible by exploiting the radiation modes of the structure. Since $n_f < n_s$, two types of radiation modes are supported according to the value of the effective refractive index n_{eff} (defined as the ratio between the propagation constant β of the mode and the wavenumber k_0): i) if $n_{\text{eff}} < n_f$, the radiation mode field profile is oscillating in the film and in the substrate, and is evanescent in the cover [12]; ii) if $n_f < n_{\text{eff}} < n_s$, the field is oscillating in the substrate, and evanescent both in the cover and in the film. We will hereafter refer to these modes respectively as type I and type II radiation modes, as shown in Fig. 1(b).

If a prism is used to couple light into the radiation modes of the dielectric structure (carrying a power P_s), the corresponding output power P_{out}, i.e., the power carried by the radiation modes after being refracted in air (see Fig. 2), turns out to depend strongly on the n_{eff} of the radiation modes themselves. The curve relating P_{out} to n_{eff} can be calculated according to a modeling of the prism-coupling process of radiation modes into planar dielectric structures. Through a least squares fitting of the experimental points to this curve, the optical parameters of the ordinary refractive index profile are then determined. The modeling proposed for the coupling process is an extension of that adopted by Tien and Ulrich for guided modes [10], and is summarized in the Appendix.

The result of the modeling is a quite complex function which relates P_{out} to the n_{eff} and to the other quantities involved in the coupling process: the waveguide depth w and the film refractive index n_f, which are the parameters to be determined by means of the least squares fitting procedure; n_p and n_s, which are the prism refractive index and the substrate ordinary index, that are supposed to be known [13], [14]; S, L, D, P_p, which are, respectively, the air-gap spacing, the length, and the width of the coupling region, the power incident on the coupling region (see Fig. 2), that are not *a priori* known. To determine the unknown parameters S, L, D, and P_p, the following considerations have been taken into account. The air spacing S affects both real and imaginary parts of the reflection and transmission coefficients at the film–gap and prism–gap interfaces, and thus significantly contributes to the behavior of the curve P_{out} versus n_{eff}. S can thus be obtained, as w and n_f, from the least squares fitting of the experimental points with the theoretical curve P_{out} versus n_{eff}. As to the length of the coupling region L, it has to be compared with the distance over which light rays reflecting back and forth in the film attenuate. If L is shorter than this distance, the interference effects tend to be smoothed, and the curve P_{out} versus n_{eff} turns out to be strongly affected by L. Actually, in practical cases, L is one order of magnitude greater than the above attenuation distance, thus concurring only to the magnitude of the coupled power without affecting the shape of the curve P_{out} versus n_{eff}. Since P_p and D also affect only the magnitude of P_{out}, it is possible to include the effects of L, D, and P_p in a single scaling factor of the curve. The least squares fitting procedure is then performed on four parameters: w, n_f, S, and the scaling factor.

To obtain a physical insight into the process of prism-coupling of ordinary radiation modes into PE waveguides, typical curves relating P_{out} to n_{eff} are reported in Fig. 3, as calculated for two different film depths, $w = 1$ μm and $w = 2$ μm, and assuming typical values for the other quantities involved. The behavior of the curves can be explained taking into account that the key factor in the coupling efficiency is the overlap between the radiation mode field profile and the evanescent field tail generated below the prism by total internal reflection of the incoming beam. Hence, when $n_{\text{eff}} > n_f$, type II radiation modes are coupled, which are evanescent both in the film and in the air gap below the prism, and P_{out} is low owing to the poor fields overlap. When the n_{eff} approaches n_f, P_{out} grows rapidly since the radiation mode field profile significantly extends also in the film region, thus increasing the fields overlap. The oscillating behavior of the coupled power when $n_{\text{eff}} < n_f$ is due to the interference between the light transmitted from the prism into the film through the air gap and the light already coupled into the film, reflecting back and forth inside the film itself, according to the Fabry–Perot behavior. The visibility of the fringes depends on the reflectivity at the film–substrate interface, which is re-

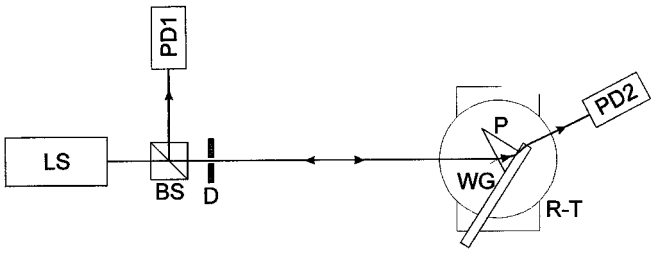

Fig. 4. Experimental setup. LS: laser, BS: beam splitter, PD1: photodetector, D: diaphragm, WG: waveguide, P: prism, R-T: motor-driven rotator and translation stages, PD2: photodetector.

lated to the index change $\Delta n = n_f - n_s$, while the distance between the different peaks is a function of the optical path length of the light reflecting back and forth in the film, and depends on the optical depth $w \cdot n_f$, thus resulting in a higher number of peaks for the deeper waveguide. Moreover, it can be observed that the slope of the curve when n_{eff} approaches n_f is steeper for the deeper waveguide.

Before going into the details of the experimental results, it is worth pointing out that the accuracy of the method relies upon the fact that the fitting is performed on the whole curve P_{out} versus n_{eff}, so as to take into account also the steep region occurring for $n_{\text{eff}} \cong n_f$, which is strongly affected by the ordinary refractive index change. Otherwise, if only the positions of maxima and minima are considered for the optical parameters reconstruction [8], [9], all the information included in this region are lost, and the accuracy in the determination of n_f becomes strongly dependent on the fringes sharpness, which cannot be resolved experimentally with sufficient precision.

III. Measurement Method and Experimental Results

The experimental setup closely resembles that normally used for m-lines spectroscopy, and is shown in Fig. 4. The prism is firmly pressed onto the waveguide which is mounted on a motor-driven stage allowing both translation and rotation. The beam splitter and photodetector 1 are used to find the orthogonality condition between the laser beam and the prism input face, which is the reference condition for the following rotations. Once this condition is found, the prism–waveguide ensemble is rotated as long as the laser beam impinges on the prism at an angle such that $n_{\text{eff}} \cong n_s$, which corresponds to the cutoff condition for radiation modes. The prism is then rotated step by step and the power coupled into radiation modes exiting the substrate is collected by photodetector 2. At each step, the prism–waveguide ensemble is translated until the best coupling efficiency is achieved, so as to keep the coupling conditions optimized during the angular scanning. To maximize the amplitude of the scanning and thus to obtain a significant number of experimental points for the index profile reconstruction, it is necessary to place the prism very close to the output face of the waveguide, thus avoiding unwanted reflection of radiation modes on the lower edge of the output face.

The method has been applied to the determination of the ordinary index profile of a PE waveguide, which, as previously stated, is assumed to be step-like. The experimental curve at $\lambda = 0.633$ μm of the power coupled into radiation modes as a function of the corresponding n_{eff} is reported in Fig. 5 together with the best fitting curve obtained by the modeling described in the Appendix. The theoretical curve closely follows the experimental points in the region of maximum slope, which is mostly responsible for the reconstructed n_f value, and also predicts very well the spacing between the interference peaks, mainly due to the optical depth $w \cdot n_f$ of the light inside the film. On the contrary, the amplitude of the interference peaks is not so well fitted, very likely owing to some disagreement with the real index profile shape, less sharp than the step-like assumed one.

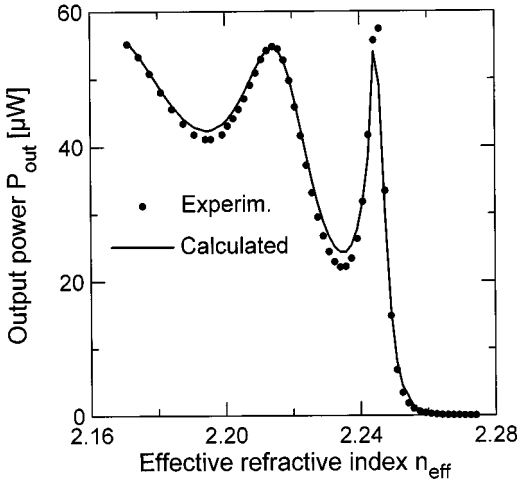

Fig. 5. Filled circles: experimental values of the power coupled into radiation modes and exiting the substrate as a function of the corresponding n_{eff}. Continuous line: fitting curve calculated according to the theory reported in the Appendix. ($\lambda = 0.633$ μm).

The values of the best fitting parameters are the following:

$$w = 1.446\ \mu\text{m} \qquad n_f = 2.2549 \qquad S = 0.028\ \mu\text{m}.$$

By repeating the measurement with different coupling conditions, the above values are found to be reproducible within 0.005 μm for w and 0.0001 for n_f. The main reason for this uncertainty in the reconstructed optical parameters is likely to come from the experimental error on the power measurements. To verify this assumption, standard statistical techniques were applied. The nonlinear relation giving the transmitted power P_{out}, at each n_{eff}, for any set of parameters w, n_f, and S, has been linearized by performing a Taylor expansion in correspondence of the best fitting parameters reported above. If a 5% uncertainty in the power measurements is assumed, which is a slight overestimate of our actual experimental error, an accuracy of 0.005 μm on w and 0.0001 on n_f is found. Actually, the discrepancy between the experimental points and the best fitting curve in Fig. 5 is in some regions greater than the claimed uncertainty in the power measurements; this is mainly due to the assumption of a step-index ordinary profile, which is indeed an approximation of the real index profile. Thus the reported accuracy does not include the error due to the slightly different index-profile shape, but refers to the reconstruction of the parameters of the best suited step-index profile, this being, however, the generally accepted approximation, sufficient in most of the applications discussed in Section I.

It is worth noting that the accuracy of the method is not significantly affected by an imprecise knowledge of the substrate refractive index n_s. Indeed, n_s comes into play in the Fresnel coefficients at the film–substrate and air–substrate interfaces, and contributes only to the fringes visibility. Thus an imprecision on the n_s value of the order of 0.0002 [14], which is our case, results in negligible variations of the reconstructed optical parameters. On the contrary, when the ordinary refractive index change $\Delta n = n_f - n_s$ is determined, the accuracy on the n_s value has to be considered and the resulting accuracy of Δn is 0.00022. In the end, when evaluating Δn for the above waveguide, a value of -0.0314 is found, equal to 0.29 times the extraordinary refractive index change, which is in good agreement with the typical factor of about one third given in the literature [11].

Further confirmation of the accuracy of the method proposed can be obtained by means of an independent measurement of the film depth. To this end, the extraordinary index profile has been characterized by standard m-lines spectroscopy at different wavelengths. Starting form the experimental values of the n_{eff} of the extraordinary guided modes, the optical parameters of the extraordinary index profile at different wavelengths have been determined, and a mean value of the depth has been calculated, equal to 1.442 μm, which is in agreement with the above reported value obtained starting from the ordinary refractive index profile within the experimental errors.

It is worth pointing out that the overall accuracy of the method further increases for deeper waveguides, while it gets lower in the case of thinner waveguides. In fact, when coupling light in deeper waveguides, the overlap between the evanescent field generated below the prism by total internal reflection and the evanescent field tail of type II radiation modes is appreciably lower, so that a steeper transition region between the two types of radiation modes occurs, as evidenced in Fig. 3, and a better discrimination of n_f is achieved. Furthermore, owing to the higher depth, the optical path length of the light inside the film is increased, and the curve P_{out} versus n_{eff} exhibits many more interference peaks (see again Fig. 3), that concur to a more accurate determination of w. On the contrary, if the waveguide is very thin, the transition between type I and type II radiation modes becomes smooth, and the interference peaks disappear. In this case, to obtain a fast and reliable convergence of the least squares fitting procedure, it is necessary to limit the fitting to three parameters only, i.e., w, n_f, and the scaling factor, by assuming a reasonable value for S. This simplification results in a lower accuracy, but, as it will be described in a future paper [15], still sufficient for a satisfactory characterization of a waveguide single mode down to the ultraviolet (UV) spectral range.

IV. Conclusions

A method for the accurate determination of the optical parameters of the ordinary refractive index profile of PE waveguides is presented and discussed. The method exploits the dependence of the behavior of the power coupled into the radiation modes, and thus of the power P_{out} exiting the substrate, on the effective indices of the radiation modes themselves. The curve relating P_{out} to n_{eff} exhibits i) a sharp slope change when the effective index of the coupled radiation mode (n_{eff}) approaches the film refractive index (n_f) and ii) an oscillatory behavior when the effective index is lower than n_f. Both features are strongly dependent on the optical parameters of the waveguide film, so that, by means of a least squares fitting of the expected curve to the experimental points, an accuracy of 0.0001 in the determination of the ordinary film refractive index and of 0.005 μm in the determination of the index profile depth can be achieved.

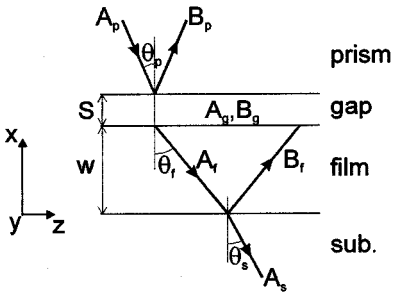

Fig. 6. Rays scheme of electromagnetic fields in a prism-coupling system in the case of an incident plane wave.

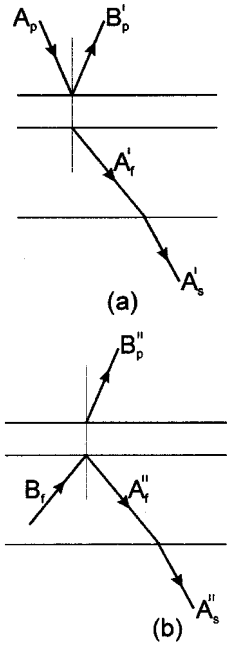

Fig. 7. Fields amplitudes involved in the calculation of (a) $t_{p-f} = A'_f/A_p$ and $t_{f-s} = A'_s/A'_f$ and (b) $r_{f-f} = A''_f/B_f$.

Appendix

To determine the relationship P_{out} versus n_{eff}, we first determine P_s versus n_{eff} by making use of the well-known Tien and Ulrich [10] prism-coupling theory, here extended, for the first time to our knowledge, to radiation modes, and then relate P_{out} to P_s through the Fresnel coefficients. To this aim, the dielectric structure of the prism-coupling system is considered as a four layers structure like that reported in Fig. 6. The different layers correspond to prism, gap, film and substrate, hereafter denoted by p, g, f, and s subscripts respectively. When coupling ordinary light in PE films, the refractive indices of the layers are such that $n_p > n_s > n_f > n_g$.

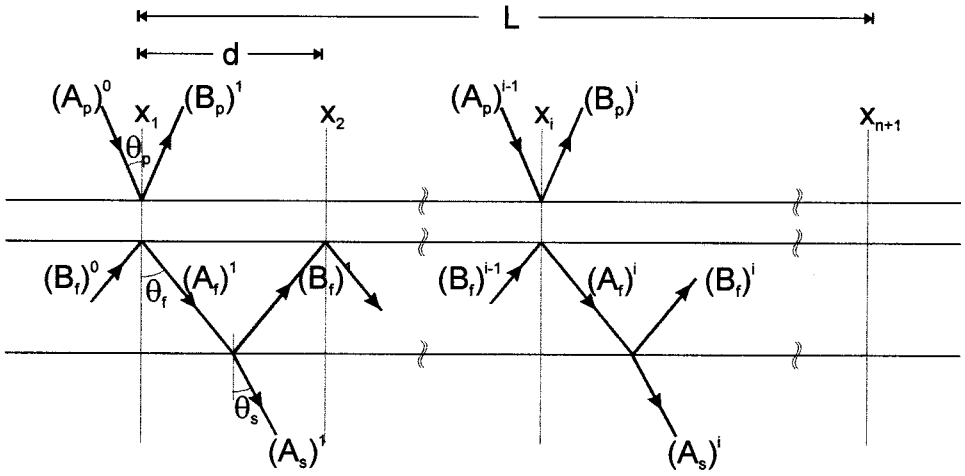

Fig. 8. Scheme of the different contributions to the substrate field A_s when the overall coupling region length is considered.

A plane wave impinging on the prism–gap interface at an angle θ_p, being partially reflected and partially transmitted through the air gap, gives rise to waves propagating in the film and in the substrate. For transverse electric (TE) polarization, which is the case of the measurements here reported, the complex electric field in the m-layer $(m = p,\ g,\ f,\ s)$ is [12]

$$E_{y,\,m} = [A_m \exp(i\gamma_m x) + B_m \exp(-i\gamma_m x)] \exp\left(i(\omega t - \beta z)\right) \tag{1}$$

where x, z is the reference axes reported in Fig. 6; ω is temporal frequency; A_m, B_m are amplitudes of downward and upward propagating plane waves respectively (with $B_s = 0$); $\beta = k_0 n_p \sin\theta_p$ is the propagation constant of the coupled mode; and $\gamma_m = k_0\sqrt{n_m^2 - n_{\text{eff}}^2}$ is the transverse wave-vector component (with k_0 = free-space wave-number and $n_{\text{eff}} = \beta/k_0$). The choice of the angle θ_p fixes both β and γ_m, and hence also the field shapes in the different layers. When θ_p is such that type I radiation modes are coupled (γ_g imaginary and γ_f, γ_s real), the electric field profile is evanescent in the gap and oscillatory in the film and in the substrate, while when type II radiation modes are coupled (γ_g, γ_f imaginary and γ_s real), the electric field is oscillatory only in the substrate region.

To determine the coupling efficiency of type I and type II radiation modes, the calculation of A_s as a function of A_p is needed. The latter is related to the power P_p incident on the coupling region by the well-known relationship

$$A_p = \sqrt{2P_p/\varepsilon_0 c n_p L \cos\theta_p D}$$

where L and D are length and width of the coupling region, respectively, and ε_0 and c are vacuum dielectric permittivity and light speed. For the calculation of A_s as a function of A_p it is necessary to analyze separately the two types of radiation mode.

Type I Radiation Modes: with reference to Fig. 7(a) and (b), A_s is given by the sum of A_s', due to the field A_p incident at the prism–gap interface and transmitted through the air gap toward the substrate, and A_s'', due to the field B_f already coupled into the film and reflected at the film–gap interface back into the substrate. A_s' and A_s'' are the fields responsible of the interference effects described in Section II. These two fields are determined by applying the boundary conditions for both electric and magnetic fields E_y and H_z at the different interfaces

$$\begin{aligned} E_{y,\,p}(x = w + S) &= E_{y,\,g}(x = w + S) \\ H_{z,\,p}(x = w + S) &= H_{z,\,g}(x = w + S) \\ E_{y,\,g}(x = w) &= E_{y,\,f}(x = w) \\ H_{z,\,g}(x = w) &= H_{z,\,f}(x = w) \\ E_{y,\,f}(x = 0) &= E_{y,\,s}(x = 0) \\ H_{z,\,f}(x = 0) &= H_{z,\,s}(x = 0) \end{aligned} \tag{2}$$

with $H_{z,\,\iota} = (i/\omega\mu)(\partial E_{y,\,\iota}/\partial x)$, in accordance with Maxwell equations since the y-dependence is negligible in planar waveguides. By solving (2) with respect to A_s', taking into account the fields of the configuration of Fig. 7(a), the transmission coefficients $t_{p-f} = A_f'/A_p$ and $t_{f-s} = A_s'/A_f'$ are obtained. Likewise, if the fields of the configuration of Fig. 7 (b) are considered, the solution of (2) gives the reflection coefficient $r_{f-f} = A_f''/B_f$. These coefficients are needed to calculate the coupled power inside the substrate P_s. To this end, the coupling region is divided into n intervals having length equal to the period of the zig-zag path of light reflecting back and forth inside the film (see Fig. 8). By denoting with θ_f the angle between the ray propagation direction and the x-axis, n results equal to L/d with $d = 2w \cdot \tan\theta_f$, and $\tan\theta_f = \beta/\gamma_f$. The A_s field amplitude in the ith interval can then be related to the incident field A_p and to the B_f field of the $(i-1)$th interval by means of the equations

$$\begin{aligned} (A_f)^i &= r_{f-f}(B_f)^{i-1} + t_{p-f}A_p \\ (A_s)^i &= t_{f-s}(A_f)^i \end{aligned} \quad \text{with} \quad i = 1, 2, \ldots, (n+1) \tag{3}$$

which can be recursively solved by imposing the initial condition $(B_f)^0 = 0$. Once the substrate field amplitudes $(A_s)^i$ are determined in all the intervals, the coupled power is calculated as the sum of the powers carried by each $(A_s)^i$ field

$$P_s = (Dd\cos\theta_s) \cdot \sum_{i=1}^{n} \left\{ \tfrac{1}{2}\varepsilon_0 c n_s \left[(A_s)^i\right]^2 \right\} \tag{4}$$

where D is the width of the coupling region and θ_s is the angle formed by the ray propagation direction in the substrate with respect to the x-axis ($\tan\theta_s = \beta/\gamma_s$).

Type II Radiation Modes: the determination of P_s is more straightforward owing to the lack of multiple reflections of the light inside the film. It is sufficient to solve (2) with reference to the Fig. 7(a) configuration of fields, taking into account that γ_f is no longer real but is imaginary. In this case, only one transmission coefficient is determined, $t_{p-s} = A_s/A_p$, giving the relationship between the substrate field and the incident field, so that P_s results to be

$$P_s = (DL\cos\theta_s)\cdot\tfrac{1}{2}\varepsilon_0 c n_s (A_s)^2 \tag{5}$$

with $A_s = t_{p-s}A_p$ depending on the n_{eff} of the coupled radiation mode.

By using (4) and (5), respectively, for type I and type II radiation modes, and, as already stated, by taking into account the Fresnel coefficient relating P_s to P_{out}, the full behavior of P_{out} versus n_{eff} is determined.

REFERENCES

[1] P. Baldi, M. P. De Micheli, K. El Hadi, S. Nouh, A. C. Cino, P. Aschieri, and D. B. Ostrowsky, "Proton exchanged waveguides in $LiNbO_3$ and $LiTaO_3$ for integrated lasers and nonlinear frequency converters," *Opt. Eng.*, vol. 37, pp. 1193–1202, 1998.

[2] M. H. Chou, J. Hauden, M. A. Arbore, and M. M. Fejer, "1.5-μm-band wavelength conversion based on difference-frequency generation in $LiNbO_3$ waveguides with integrated coupling structures," *Opt. Lett.*, vol. 23, pp. 1004–1006, 1998.

[3] J. L. Jackel, C. E. Rice, and J. J. Veselka, "Proton exchange for high-index waveguides in $LiNbO_3$," *Appl. Phys. Lett.*, vol. 41, pp. 607–608, 1982.

[4] Y. N. Korkishko, V. A. Fedorov, M. P. De Micheli, P. Baldi, K. El Hadi, and A. Leycuras, "Relationship between structural and optical properties of proton-exchanged waveguides on Z-cut lithium niobate," *Appl. Opt.*, vol. 35, pp. 7056–7060, 1996.

[5] S. Chao, Y.-C. Chen, and H.-Y. Chen, "Determination of ordinary refractive index profile for a planar waveguide by transmission spectrum analysis," *J. Appl. Phys.*, vol. 83, pp. 5650–5657, 1998.

[6] L. W. Walpita, "Solution for planar optical waveguide equations by selecting zero elements in a characteristic matrix," *J. Opt. Soc. Amer.*, vol. 2, pp. 595–602, 1985.

[7] K. El Hadi, P. Baldi, M. P. De Micheli, D. B. Ostrowsky, Y. N. Korkishko, V. A. Fedorov, and A. V. Kondrat'ev, "Ordinary and extraordinary waveguides realized by reverse proton exchange on $LiTaO_3$," *Opt. Commun.*, vol. 140, pp. 23–26, 1997.

[8] P. J. Chandler, F. Lama, P. D. Townsend, and L. Zhang, "Analysis of doped layer step waveguides using dark modes," *IEEE J. Lightwave Technol.*, vol. 8, pp. 917–920, 1990.

[9] J. Olivares, M. A. Diaz-Garcia, and J. M. Cabrera, "Direct measurement of ordinary refractive index of proton exchanged $LiNbO_3$ waveguides," *Opt. Commun.*, vol. 92, pp. 40–44, 1992.

[10] P. K. Tien and R. Ulrich, "Theory of prism-film coupler and thin-film light guides," *J. Opt. Soc. Amer.*, vol. 60, pp. 1325–1337, 1970.

[11] J. F. Offersgaard, T. Veng, and T. Skettrup, "Accurate method for determining the refractive-index profiles of planar waveguides in uniaxial media with the optical axis normal to the surface," *Appl. Opt.*, vol. 35, pp. 2602–2609, 1996.

[12] D. Marcuse, *Theory of Dielectric Optical Waveguides*. New York and London: Academic, 1974, pp. 19–30.

[13] R. Ramponi, M. Marangoni, R. Osellame, and V. Russo, "Use of radiation and hybrid modes to increase the accuracy in the determination of the refractive indices of rutile," *Appl. Opt.*, vol. 39, pp. 1–6, 2000.

[14] G. J. Edwards and M. Lawrence, "A temperature-dependent dispersion equation for congruently grown lithium niobate," *Opt. Quantum Electron.*, vol. 16, pp. 373–374, 1984.

[15] R. Ramponi, M. Marangoni, R. Osellame, and V. Russo, to be published.

M. Marangoni, photograph and biography not available at the time of publication.

R. Ramponi, photograph and biography not available at the time of publication.

R. Osellame, photograph and biography not available at the time of publication.

V. Russo, photograph and biography not available at the time of publication.